Biophysical Journal, Volume 99

Supporting Material

Authors: Rajiv Jesudason, Susumu Sato, Harikrishnan Parameswaran, Ascanio Araujo, Arnab Majumdar, Philip Allen, Erzsebet Bartolak-Suki, and Bela Suki

Title: MECHANICAL FORCES REGULATE ELASTASE ACTIVITY AND BINDING SITE AVAILABILITY IN LUNG ELASTIN

Experiments

Enzyme activity assay

The activity of porcine pancreatic elastase (PPE) and its fluorescent labeled form (*f*-PPE) was quantified using the ENZChek elastase activity assay kit (Molecular Probes, Eugene, OR) based on the manufacturer's instructions. An amount of 50µl of reaction buffer was added to each well of a 96 well-plate followed by addition of 50µl of 100µg/mL DQ elastin to each well. The *f*-PPE and PPE was then added to designated wells at a final concentration of 3 or 6µg/µl. The plate was then incubated at room temperature and monitored in a SpectraMax Plus384 micro-plate reader (Molecular Devices, Inc. Sunnyvale, CA). The samples were excited at 505 nm and emitted at 515 nm and fluorescent intensity measurements were taken in 10 minute intervals.

The results of the activity assay are shown in Figure S1. An increase in fluorescent intensity corresponds to active enzyme cleaving the substrate and yielding fluorescent fragments. As shown, the control fluorescence remained fairly constant throughout the measurement period indicating no substrate fragment production. As expected, introduction of unlabeled PPE (squares) resulted in an effective increase in fluorescent intensity with time. A similar increasing trend was exhibited with the introduction of *f*-PPE (crosses) of the same concentration. As described in the main text, there was an average loss of activity of 18% due to fluorescent tagging of PPE ($p<0.03$).

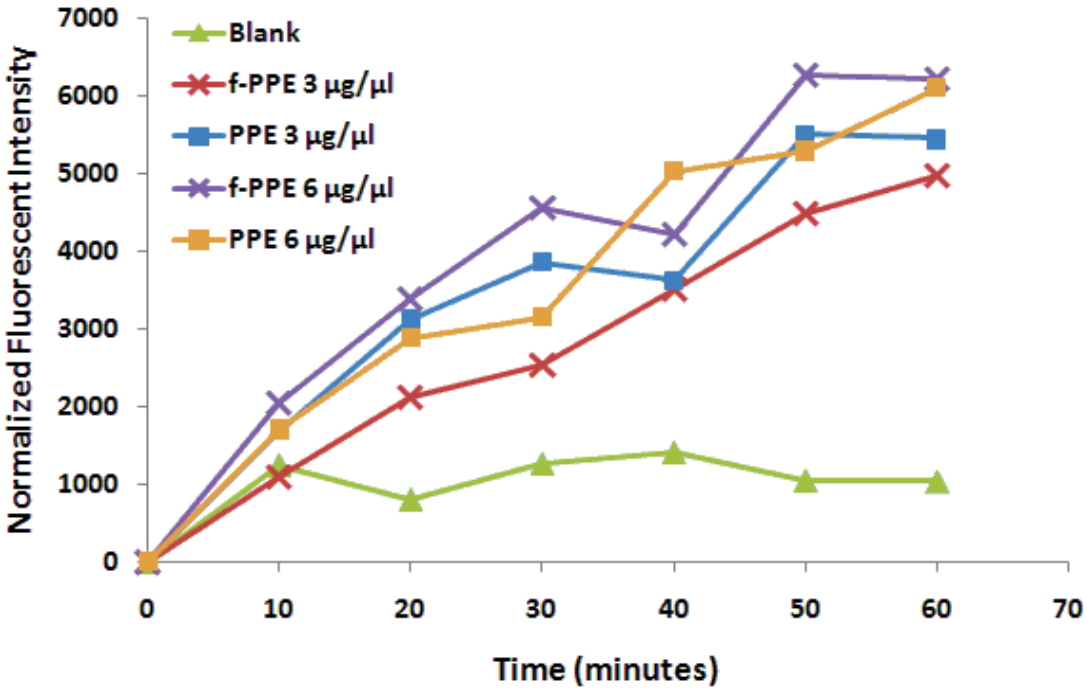

Figure S1: Kinetic results of the Elastase Activity Assay. Fluorescence was normalized by the baseline value at time 0. The *f*-PPE wells are denoted by crosses, while the PPE wells are shown by squares.

Effect of temperature and fluorescence labeling on mechanics

A functional assay of elastase activity based on the mechanics protocol described in the Methods and outlined in Figure 1B was repeated with the use of *f*-PPE. The changes in mechanical properties induced by *f*-PPE were compared to that of unlabeled PPE. Figure S2 displays the results of the mechanics protocol, comparing the effects of PPE (dashed lines) and *f*-PPE (solid lines). As the data shows, *f*-PPE induced similar trends to those of the PPE. However, the rates of modulus decrease were slower and less severe than with PPE. As described in the main text, the differences are not substantial (9.1%), but statistically significant ($p<0.001$). Since the mechanics assays were done at body temperature whereas imaging was carried out at room temperature, the digestion using *f*-PPE was repeated at room temperature (red solid line). The *f*-PPE digestion at room temperature resulted in a slower decrease in the normalized modulus and the drop in modulus at time 60 min. was significantly different the PPE digestion at body temperature ($p<0.05$).

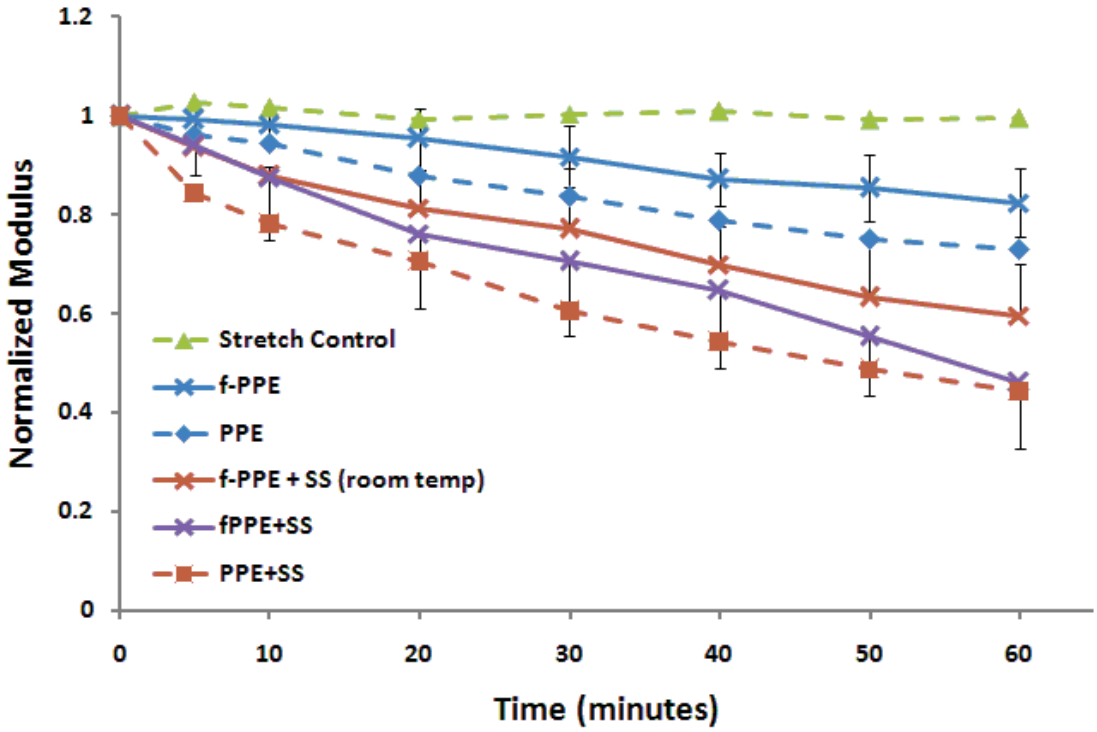

Figure S2: Means and SDs of the normalized Young's modulus as a function of time for tissues treated with PPE (dashed lines) and *f*-PPE (solid lines) respectively, with and without static stretch (SS). *f*-PPE: n=3, *f*-PPE+SS: n=4, *f*-PPE+SS at room temp: n=3.

Models

Network model

The purpose of the network model of the lung tissue strip is to estimate the average strain on alveolar walls, the microstrain, as a function of macroscopic strain. The details of the model are presented in the main text.

At each strain level, we separated springs that were within two-hop distance of the boundary (boundary springs), and those further than two-hop distance from the boundary were considered to be interior springs. Individual strains for boundary springs that were within 20 degrees of the direction of macroscopic strain were recorded. These values were then used to calculate the mean and standard deviation of the micro strain as a function of macro strain shown in Figure 3 in the main text. The configurations of the network at 0, 40% and 80% strains are shown in Figure S3.

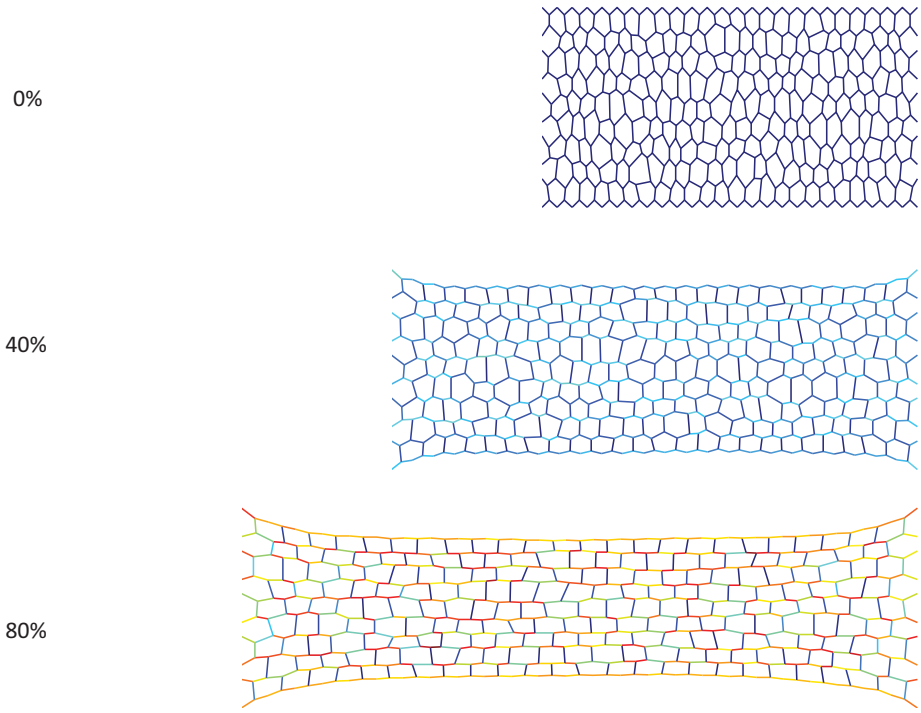

Figure S3: Hexagonal network model at mechanical equilibrium under 0%, 40% and 80% macroscopic uniaxial strains. Segments are colored according to their local microscopic strain, blue representing low and red high strain. The same coloring scheme was applied to all three networks.

Time-course of fluorescence recovery after photobleach

To model the FRAP process, we first assume that the reaction-diffusion process is in equilibrium throughout. At $t=t_B$, a small region R_B is exposed to intense laser radiation which bleaches all fluorescent enzymes, free and bound, inside that region. This process converts **E** and **EB** to their bleached, non-fluorescing species **E*** and **EB***,

$$\left.\begin{array}{l}\mathbf{E}\rightarrow\mathbf{E}^{*}\\ \mathbf{EB}\rightarrow\mathbf{EB}^{*}\end{array}\right\}\quad \text{inside } R_B$$

Following the bleaching process, the bleached species participate in an additional reaction pathway. The set of reactions for $t>t_B$, is given by

$$\mathbf{E}+\mathbf{B}\xrightarrow{k_{on}}\mathbf{EB}\xrightarrow{k_{off}}\mathbf{E}+\mathbf{B}$$

$$\mathbf{E}^{*}+\mathbf{B}\xrightarrow{k_{on}}\mathbf{EB}^{*}\xrightarrow{k_{off}}\mathbf{E}^{*}+\mathbf{B}$$

We note that the bleaching occurs within R_B and thus for times immediately following the bleach, the bleached species are only within R_B. However the free bleached enzyme **E*** soon diffuses out of R_B. The bleached enzymes can then bind to binding sites outside R_B, creating new **EB*** outside R_B. Simultaneously the bound bleached species **EB*** inside R_B dissociate and the free bleached enzymes can diffuse outside R_B. The evolution of the

concentrations of the five species involved is governed by the following set of coupled reaction-diffusion equations:

$$\frac{\partial E}{\partial t} = D\,\nabla^2 E - k_{\text{on}}\,E\,B + k_{\text{off}}\,EB$$

$$\frac{\partial E^*}{\partial t} = D\,\nabla^2 E^* - k_{\text{on}}\,E^*\,B + k_{\text{off}}\,EB^*$$

$$\frac{\partial B}{\partial t} = -k_{\text{on}}\,E\,B - k_{\text{on}}\,E^*\,B + k_{\text{off}}\,EB + k_{\text{off}}\,EB^*$$

$$\frac{\partial EB}{\partial t} = k_{\text{on}}\,E\,B - k_{\text{off}}\,EB$$

$$\frac{\partial EB^*}{\partial t} = k_{\text{on}}\,E^*\,B - k_{\text{off}}\,EB^*$$

The fluorescence measured in the region R_B drops to 0 at $t=t_B$ and slowly recovers for $t>t_B$. This fluorescence

$$FRAP(t) = \int_{R_B}(E + EB)$$

is the total amount of fluorescent enzyme, bound and unbound, in the region R_B.

Simulation of FRAP

In order to simulate the FRAP process, we set up a model system consisting of a rectangular fiber embedded in a circular airspace (Figure S4). We assumed that the normalized binding site density β on the fiber is large compared to the initial enzyme density η. Thus, the free binding site density B is much larger than the unbound and bound enzyme densities E and EB, respectively, and is essentially constant throughout the recovery process. This decouples the evolution of the bleached enzymes and renders the evolution equations linear. The equations of interest can thus be written as,

$$\frac{\partial E}{\partial t} = D\,\nabla^2 E - k_{\text{on}}^*\,E + k_{\text{off}}\,EB$$

$$\frac{\partial EB}{\partial t} = k_{\text{on}}^*\,E - k_{\text{off}}\,EB$$

where $k_{\text{on}}^* \equiv k_{\text{on}}\,B$ is the apparent on rate. This system was then solved using Matlab's partial differential equation toolbox. First, a unit concentration of enzyme particles was placed in the circle except the fiber. The equilibrium condition of the system was then obtained so that the fiber took up some particle via binding and consequently the free enzyme concentration in the fluid phase decreased. Next, a circular bleach spot R_B was created by setting the bound and unbound enzyme concentrations inside R_B and the system was solved again. The first image on Figure S4 shows the system immediately after the bleach spot was created and the second and third images are the system configuration at 2 later time points. It can be also seen that due to binding, the enzyme concentration is much higher on the fiber than in the fluid phase.

Once the system was solved, *FRAP(t)* was measured as shown in Figure S5 (top). We then used the model form

$$FRAP(t) = 1 - C_{\text{eq}}\, e^{-k_{\text{off}}\, t}$$

to fit the measured data, by fitting a straight line to log*(1-frap(t))* as shown in Figure S5 (bottom). Sprague *et al.* (1) derive the constant

$$C_{\text{eq}} \equiv \frac{k_{\text{on}}^{*}}{k_{\text{on}}^{*} + k_{\text{off}}}$$

which can thus be used to recover k_{on}^{*}.

The results in Figure S5 (bottom) demonstrate that we can estimate the true values of k_{off} and k_{on}^{*} within an error of 7% when the diffusion constant is at least 10 times k_{on}^{*}.

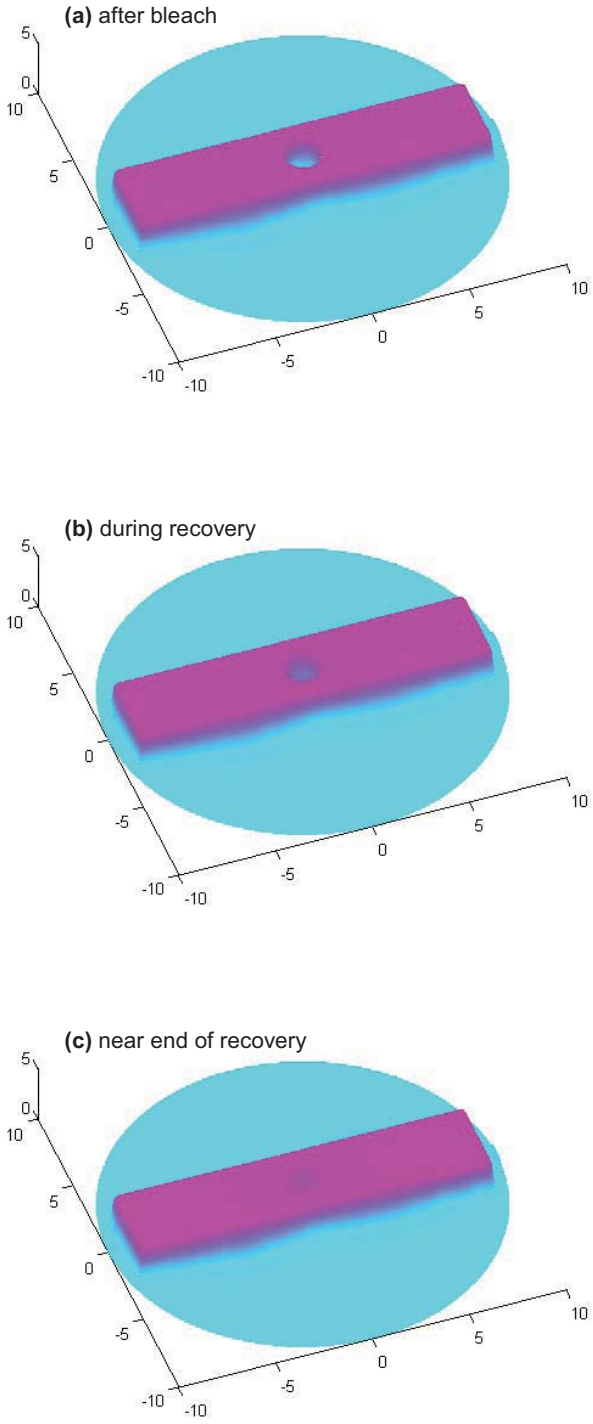

Figure S4: Simulation of the FRAP process showing the density of bound fluorescent enzymes on a rectangular fiber shown in pink within in a circular airspace. The central hole with a diameter half of the diameter of the fiber corresponds to the bleached region over which fluorescence recovers in time. Color is proportional to enzyme concentration (red high, blue low) showing strong binding of the enzyme to the fiber.

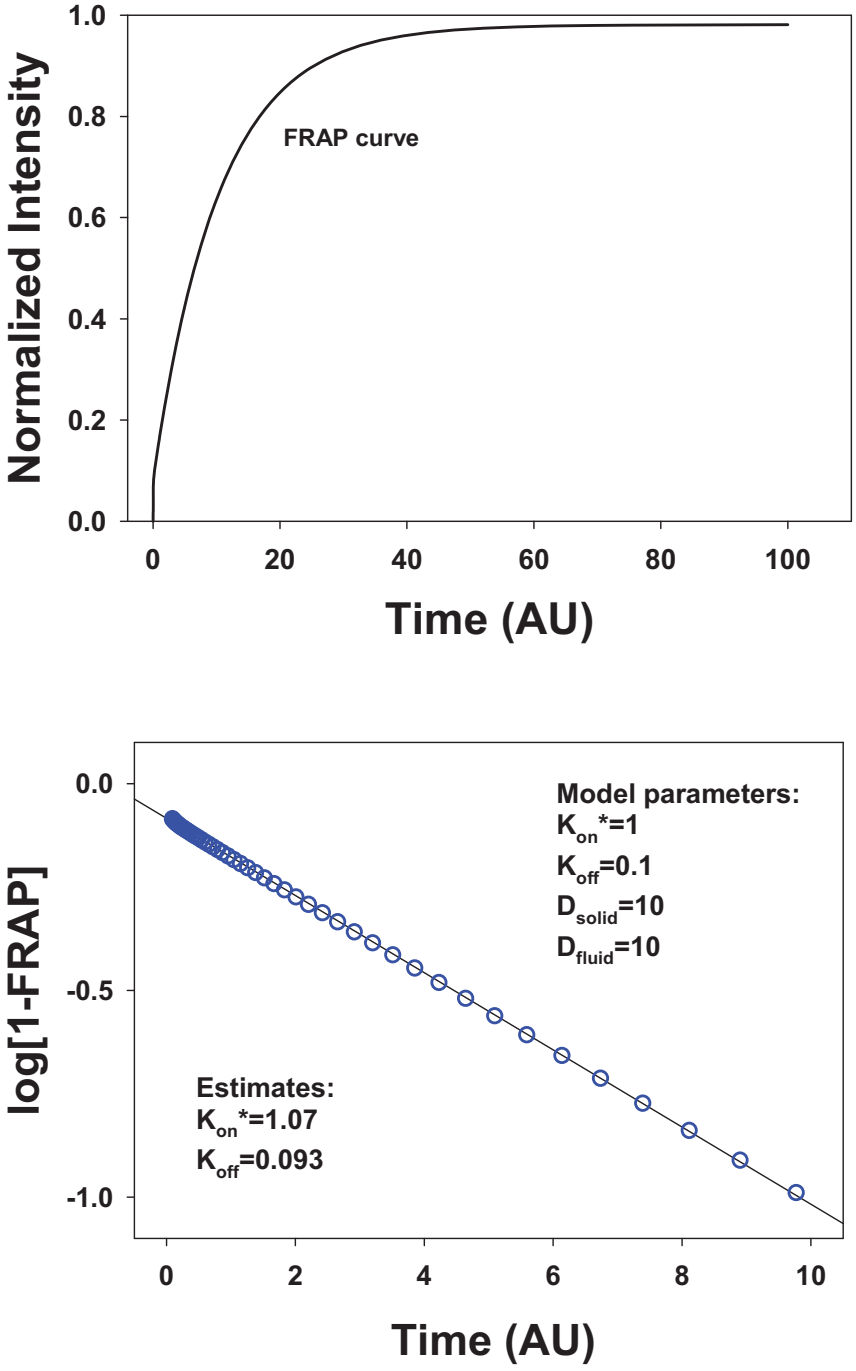

Figure S5: Simulated fluorescence recovery after photobleaching showing the recovery of the integrated fluorescent intensity *FRAP(t)* in the bleached region as a function of time (top), and the straight line fit to *log[1-FRAP(t)]*.

References

1. Sprague, B. L., R. L. Pego, D. A. Stavreva, and J. G. McNally. 2004. Analysis of binding reactions by fluorescence recovery after photobleaching. Biophys J 86:3473-3495.